ELSEVIER

Journal of Structural Geology 28 (2006) 1835–1848

JOURNAL OF STRUCTURAL GEOLOGY

www.elsevier.com/locate/jsg

The problem of area change in tangential longitudinal strain folding

N.C. Bobillo-Ares [a], J. Aller [b,*], F. Bastida [b], R.J. Lisle [c], N.C. Toimil [c]

[a] *Departamento de Matemáticas, Universidad de Oviedo, 33005 Oviedo, Spain*
[b] *Departamento de Geología, Universidad de Oviedo, Jesus Arias de Velasco s/n, 33005 Oviedo, Asturias, Spain*
[c] *School of Earth, Ocean and Planetary Sciences, Cardiff University, CF10 3YE, UK*

Received 28 November 2005; received in revised form 26 June 2006; accepted 17 July 2006
Available online 1 September 2006

Abstract

This paper deals with some problems with the concept and properties of the folding mechanism named tangential longitudinal strain. A general two-dimensional mathematical description of this mechanism in terms of displacements and finite strains is presented. In the analysis of this mechanism of folding, two geologically reasonable variants are considered. The first of these, referred to as parallel tangential longitudinal strain folding, involves no finite elongation of lines perpendicular to the layer and produces class 1B (parallel) folds. The second variant is characterized by the conservation of area across the fold profile and is therefore termed equiareal tangential longitudinal strain folding; it produces folds ranging from class 1B to more complex shapes with the development of a bulge in the hinge zone inner arc when amplitude and curvature are high. Using the computer program ''FoldModeler'' which incorporates the derived equations for displacements and finite strains, the geometrical features of idealized folds produced by these two variants have been studied, together with those arising from their successive or simultaneous combination. The implications of the operation of these two deformation mechanisms in natural folds are then considered and a discussion is presented about the features that can be diagnostic of their operation in nature. It is suggested that the two mechanisms operate together in the formation of natural folds, in a way that deformation probably begins with equiareal tangential longitudinal strain, but subsequently gives way to parallel tangential longitudinal strain when strain concentration in some parts of the folded layer makes area change probable.

Keywords: Folding; Minor structures; Structural geology; Tangential longitudinal strain

1. Introduction

Definition of the folding mechanism referred to as ''tangential longitudinal strain'' (Ramsay, 1967, p. 397) is based on the well-known fact that when a competent layer is folded, lines parallel to the layer boundaries increase or decrease in length depending on their position near the outer or the inner arc, respectively (cf. Kuenen and de Sitter, 1938). Separating the zones of tangential extension and tangential shortening is a surface made up of points with zero finite strain or neutral surface (neutral line in two dimensions). These properties can be easily demonstrated by the distortion of an initially square grid inscribed on the profile plane of a flexed rubber layer. Moreover, it is observed that straight lines normal to the folded layer boundaries remain approximately straight and normal to the boundaries during folding. These simple results illustrate in a general way the phenomenon of ''tangential longitudinal strain'' folding.

Mathematical modelling of this mechanism, intended to determine the detailed strain distribution inside the folded layer

* Corresponding author. Tel.: +34 985 103119; fax: +34 985 103103.
E-mail address: aller@geol.uniovi.es (J. Aller).

0191-8141/$ - see front matter © 2006 Elsevier Ltd. All rights reserved.
doi:10.1016/j.jsg.2006.07.004

and its structural consequences, is not a simple task and poses at present some important questions that remain unsolved. Ramberg (1961) was one of the first authors to study this mechanism and he named it ''concentric longitudinal strain''. According to him, it would dominate deformation in the hinge zone of folds, and it was quantitatively compared with ''concentric shear strain'' (or ''flexural-flow'' of Ramsay, 1967, p. 392), that would control deformation on the fold limbs. In the model developed by Ramberg (1961) no restriction is made about area change during deformation (see for example his Fig. 1); this author uses as a starting point the result obtained by Timoshenko (1940, pp. 38 and 115) in the theory of beams in pure bending (i.e. in conditions of no concentric shear strain), concentric longitudinal strain depends on the distance to the neutral surface. The main conclusion obtained by Ramberg (1961) is that strain produced by concentric shear on the limbs is negligible when compared with concentric longitudinal strain in the hinge zone for beds of homogeneous rock and where the ratio of competent layer thickness to fold wavelength is not high. These results agree with those obtained subsequently by other authors (Hudleston et al., 1996; Toimil, 2005).

Ramsay (1967, pp. 397–411) and Ramsay and Huber (1987, pp. 457–462) made a detailed study of tangential longitudinal strain. In their model for this mechanism, lines initially normal to the fold boundaries remain approximately normal after folding, and area is preserved in all parts of the folded layer profile. Assuming these two conditions (with both of them holding exactly), these authors concluded that the absolute value of the tangential extension at points on a normal to the neutral line equals the product of the curvature of this line and the distance from it. Nevertheless, these two conditions are mutually incompatible, since area conservation implies a thickness variation of the sub-layers above and below the neutral line proportional to the variation in curvature of this line. This thickness variation leads to the distortion of lines initially normal to layer boundaries, so that their orthogonal relationship is lost during folding (Ramsay, 1967, Figs. 7–63). Due to this, the analysis only provides approximate results.

Bobillo-Ares et al. (2000) developed in detail another variant of a constant area model for tangential longitudinal strain. The only condition imposed on their model is that lines originally straight and normal to the neutral line and the layer boundaries remain straight and normal to the neutral line as folding progresses. A consequence of this model is that the axes of the strain ellipse at points along the layer boundaries are not exactly tangential and normal to these boundaries, but show a small deviation that increases as the variation in curvature of the neutral line increases. This means that some shear strain exists in general along the layer boundaries, and perpendicularity between the tangent to the layer boundary and lines originally normal to it is lost.

In order to improve the models of tangential longitudinal strain, it must be taken into account that many features of natural folds suggest the existence of area change during operation of this mechanism; e.g. mineralized radial veins widening towards the outer arc in the hinge zone indicate area increase during folding, or convergent pressure solution cleavage patterns in the inner arc suggest area decrease. Models of tangential longitudinal strain with area change have been proposed by Hudleston and Holst (1984), Hudleston and Tabor (1988), Hudleston and Srivastava (1997), and Ormand and Hudleston (2003), who consider the possibility of area reduction due to pressure solution in the inner arc and re-precipitation with area increase in the outer arc. These authors propose models of tangential longitudinal strain in which: (a) the principal directions of strain are always tangential and normal to the layer boundaries and (b) the distance from any point of the folded layer to the neutral line remains constant during folding, which implies generation of a perfect parallel fold. Two variants of this model are: ''inner arc collapse'' (Hudleston and Tabor, 1988; Hudleston and Srivastava, 1997) and ''outer-arc stretching'' (Ormand and Hudleston, 2003), characterized by the location of the neutral line in the outer arc or the inner arc, respectively. However, the kinematic properties of these models have not been analysed. This analysis would be very interesting in order to compare the results with those obtained for the model of tangential longitudinal strain without area change, and would allow the combination of both models to obtain theoretical folds more similar to those found in rocks.

In this study, we develop a general mathematical model for folding by tangential longitudinal strain in two dimensions with or without area change. Then, several particular geologically reasonable cases will be considered, for which the

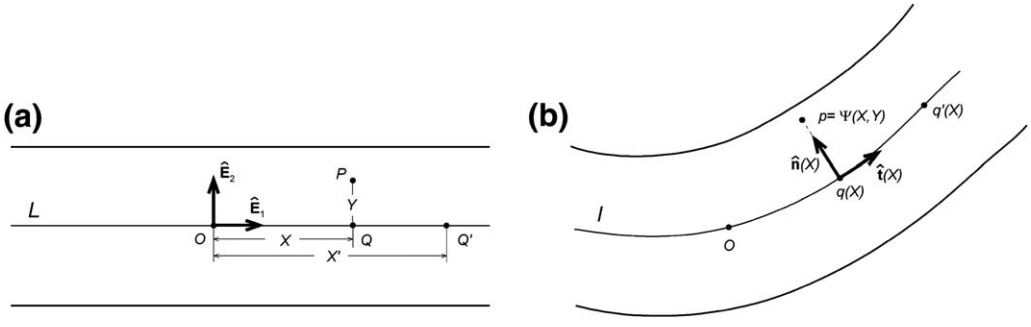

Fig. 1. Initial (a) and final (b) configuration showing the transformation of a general point $P-p$ with folding and the general ($\hat{\mathbf{E}}_1$, $\hat{\mathbf{E}}_2$) and local ($\hat{\mathbf{t}}$, $\hat{\mathbf{n}}$) reference systems. L and l are the neutral lines in the initial and final configurations, respectively.

models with and without area change are compared in order to identify the diagnostic features that could allow the discrimination of these two mechanisms in natural folds. Finally, a model will be presented in which both types of tangential longitudinal strain can be combined in successive or simultaneous superposition in order to obtain theoretical folds that provide the best fit to natural folds. The notation used in the theoretical analysis is shown in Table 1.

2. Definition of tangential longitudinal strain (TLS)

Let us consider an initially planar layer that deforms to a final folded form (Fig. 1). The main conditions that characterize TLS are (a) the existence of a ''neutral line'' (L in the undeformed state and l in the deformed state) whose points have no finite strain and (b) straight lines perpendicular to the neutral line in the original state remain straight and normal to it in the final configuration. In the present analysis, the neutral line stays attached to the same material points throughout deformation. A particle that initially occupies the point P can be located after folding using this procedure:

1. We determine the base point Q, which is the intersection point of the neutral line L and the perpendicular to it drawn from the point P (Fig. 1a).
2. We locate the point q, the deformed position of the initial point Q, on l (Fig. 1b).
3. At this point q, we consider the unit vector $\widehat{\mathbf{n}}$, perpendicular to l and pointing towards the inner arc of the folded layer.
4. Finally, the point p, the deformed position of P, is located by specifying the coefficient d so that [see Appendix A, Eq. (A1)]:

$$p = q + d\widehat{\mathbf{n}}. \tag{1}$$

Any TLS is characterized by specifying the image l of the neutral line L and the value of the coefficient d for any point P of the initial layer. Particular cases of TLS can be defined using a function $d(X, Y)$ that gives a d value for any point (X, Y) of the folded layer. Nevertheless, among all the possible d functions fulfilling condition (1) and the basic requirements of TLS, many will give rise to improbable fold shapes in geological bodies.

Table 1
Symbols and abbreviations used in the text

C_{ij}: components of the Green tensor in the basis E.
C_P: Green tensor at point P.
$d_1(X,Y) = \frac{\partial}{\partial X} d(X,Y)$.
$d_2(X,Y) = \frac{\partial}{\partial Y} d(X,Y)$.
$E = (\widehat{\mathbf{E}}_1, \widehat{\mathbf{E}}_2)$: orthonormal vector basis for the initial configuration.
ETLS: equiareal tangential longitudinal strain.
G_{ij}: elements of the Gram matrix associated with the vector basis E.
I_1, I_2: Invariants of the Green finite strain tensor at point P.
$J(X, Y)$: area ratio (final area/initial area).
L: neutral line in the initial configuration.
l: neutral line in the deformed configuration.
$\widehat{\mathbf{n}}(X)$: unit vector normal to the neutral line at X.
PTLS: parallel tangential longitudinal strain.
P, Q…: points in the initial configuration.
p, q…: points in the deformed configuration.
R: strain ratio $\left(R = \frac{\sqrt{\lambda_1}}{\sqrt{\lambda_2}}\right)$.
$S(\mathbf{a}, \mathbf{b})$: oriented area of the parallelogram ($\mathbf{a}$, $\mathbf{b}$).
TLS: tangential longitudinal strain.
$\widehat{\mathbf{t}}(X)$: unit vector tangent to the neutral line at X.
Δ: dilation.
δ_{ij}: Kronecker delta ($\delta_{11} = \delta_{22} = 1$, $\delta_{12} = \delta_{21} = 0$).
$\kappa(X)$: curvature of the neutral line at X.
λ_1, λ_2: principal quadratic elongations.
$\rho(X) = 1/\kappa(X)$: radius of curvature of the neutral line at X.

3. Analysis of TLS

We choose a point O on the neutral line L as origin of the coordinate system (Fig. 1a). Let $\widehat{\mathbf{E}}_2$ be a unit vector perpendicular to L and heading from the neutral line L towards the inner arc. $\widehat{\mathbf{E}}_1$ is a unit vector perpendicular to $\widehat{\mathbf{E}}_2$ in such a direction that the basis $E = (\widehat{\mathbf{E}}_1, \widehat{\mathbf{E}}_2)$ is a direct one.

For an arbitrary point P with coordinates (X, Y), we have:

$$\overrightarrow{OP} = X\widehat{\mathbf{E}}_1 + Y\widehat{\mathbf{E}}_2, \tag{2}$$

and, for its base point Q:

$$\overrightarrow{OQ} = X\widehat{\mathbf{E}}_1. \tag{3}$$

In this coordinate system, the fundamental equation (1) defining TLS can be written in the form:

$$p = \psi(X,Y) = \varphi(X) + d(X,Y)\widehat{\mathbf{n}}(X), \tag{4}$$

where (X, Y) are the coordinates of point P, $\psi(X, Y)$ is the deformed position of P, $\varphi(X)$ is the deformed position of Q, $d(X, Y)$ is the coefficient that defines the position of point p along the straight line normal to l at point $\varphi(X)$, and $\widehat{\mathbf{n}}(X)$ is the normal unit vector at $q = \varphi(X)$.

The coordinate X allows the straightforward measurement of distances along the neutral line L. The distance between points $Q = O + X\widehat{\mathbf{E}}_1$ and $Q' = O + X'\widehat{\mathbf{E}}_1$ is $|X' - X|$.

Due to the neutral character of the line L, the variable X in function $\varphi(X)$ also measures the arc length on the image curve l. Then, the tangent unit vector $\widehat{\mathbf{t}}(X)$ at $q = \varphi(X)$ can be obtained by direct differentiation:

$$\widehat{\mathbf{t}}(X) = \varphi'(X). \tag{5}$$

The direction chosen for vector $\mathbf{E}_1$ guarantees a positive orientation of the orthonormal basis $(\widehat{\mathbf{t}}(X), \widehat{\mathbf{n}}(X))$. The vectors $\widehat{\mathbf{t}}(X)$ and $\widehat{\mathbf{n}}(X)$ are related to their derivatives by the well known Frenet formulae:

$$\widehat{\mathbf{t}}'(X) = \kappa(X)\widehat{\mathbf{n}}(X), \tag{6}$$

$$\widehat{\mathbf{n}}'(X) = -\kappa(X)\widehat{\mathbf{t}}(X). \tag{7}$$

The function $\kappa(X)$ is the curvature at point $\varphi(X)$. By convention we put $\kappa(X) \geq 0$. Therefore, the radius of curvature $\rho(X) = 1/\kappa(X)$ is also positive.

4. Deformation gradient

At point P with coordinates (X, Y), the deformation gradient of the transformation $p = \psi(X, Y)$ is the linear operator ψ'_P that, for every vector $\mathbf{V} = V_1\widehat{\mathbf{E}}_1 + V_2\widehat{\mathbf{E}}_2$, assigns the vector:

$$\psi'_P(\mathbf{V}) = \frac{\mathrm{d}}{\mathrm{d}\beta}\psi(X+\beta V_1, Y+\beta V_2)\bigg|_{\beta=0}. \tag{8}$$

Like any other operator, the gradient is completely characterized at a point by the image vectors of the base vectors:

$$\psi'_P(\widehat{\mathbf{E}}_1) = \frac{\partial p}{\partial X},\ \psi'_P(\widehat{\mathbf{E}}_2) = \frac{\partial p}{\partial Y}. \tag{9}$$

Differentiating Eq. (4) we immediately obtain the relations:

$$\frac{\partial p}{\partial X} = \varphi'(X) + d_1(X,Y)\widehat{\mathbf{n}}(X) + d(X,Y)\widehat{\mathbf{n}}'(X), \tag{10}$$

$$\frac{\partial p}{\partial Y} = d_2(X,Y)\widehat{\mathbf{n}}(X), \tag{11}$$

where $d_1(X, Y)$ and $d_2(X, Y)$ are the partial derivatives of d computed at point P with respect to the first and the second arguments, respectively. Taking into account the Frenet equation (7), we finally obtain:

$$\frac{\partial p}{\partial X} = (1-\kappa(X)d(X,Y))\widehat{\mathbf{t}}(X) + d_1(X,Y)\widehat{\mathbf{n}}(X), \tag{12}$$

$$\frac{\partial p}{\partial Y} = d_2(X,Y)\widehat{\mathbf{n}}(X). \tag{13}$$

5. Area ratio

Let us consider the vector basis $(\widehat{\mathbf{E}}_1, \widehat{\mathbf{E}}_2)$ positioned at point P. The associated area is $S(\widehat{\mathbf{E}}_1, \widehat{\mathbf{E}}_2)$ [Appendix A, Eq. (A2)]. The respective images $(\partial p/\partial X, \partial p/\partial Y)$ characterize a parallelogram with area $S(\partial p/\partial X, \partial p/\partial Y)$. We define the area ratio by the quotient:

$$J(X,Y) = \frac{S\left(\frac{\partial p}{\partial X}, \frac{\partial p}{\partial Y}\right)}{S(\widehat{\mathbf{E}}_1, \widehat{\mathbf{E}}_2)}. \tag{14}$$

Taking into account that real transformations cannot change the orientation of a parallelogram, we have the condition:

$$J(X,Y) > 0. \tag{15}$$

Obviously, the null value must be excluded as well.

Using the result Eq. (2), from Eqs. (12) and (13) we obtain:

$$J(X,Y) = \begin{vmatrix} 1-\kappa(X)d(X,Y) & 0 \\ d_1(X,Y) & d_2(X,Y) \end{vmatrix} \frac{S(\widehat{\mathbf{t}}(X), \widehat{\mathbf{n}}(X))}{S(\widehat{\mathbf{E}}_1, \widehat{\mathbf{E}}_2)}. \tag{16}$$

Thanks to the form we have chosen for the basis $E = S(\widehat{\mathbf{E}}_1, \widehat{\mathbf{E}}_2)$, the oriented area ratio of the second factor is $+1$. So, the equation of area ratio for TLS is:

$$J(X,Y) = (1-\kappa(X)d(X,Y))d_2(X,Y). \tag{17}$$

The direction chosen for vector $\widehat{\mathbf{n}}(X)$ imposes that function $d(X, Y)$ is strictly increasing for the variable Y, for every X. Thus, $d_2(X, Y)$ has to be positive. Taking into account also the condition (15) and the Eq. (17), we obtain a limit for the values of $d(X, Y)$:

$$d(X,Y) < \frac{1}{\kappa(X)} = \rho(X). \tag{18}$$

6. Principal values and directions of strain

The analysis of the longitudinal strain in different directions is carried out by the tensor field C_P, a symmetric bilinear function at every point P:

$$C_P(\mathbf{V},\mathbf{W}) = \psi'_P(\mathbf{V})\psi'_P(\mathbf{W}). \tag{19}$$

In the basis E, C_P is represented by a matrix whose elements are the quantities:

$$C_{ij}(X,Y) = \psi'_P(\widehat{\mathbf{E}}_i)\psi'_P(\widehat{\mathbf{E}}_j). \tag{20}$$

From Eqs. (12) and (13), we immediately obtain:

$$C_{11}(X,Y) = (1-\kappa(X)d(X,Y))^2 + d_1(X,Y)^2, \tag{21}$$

$$C_{22}(X,Y) = d_2(X,Y)^2, \tag{22}$$

$$C_{12}(X,Y) = d_1(X,Y)d_2(X,Y). \tag{23}$$

The principal value λ (quadratic elongation) and the principal vector $\mathbf{V} = V_1\widehat{\mathbf{E}}_1 + V_2\widehat{\mathbf{E}}_2$ are computed solving the system of two linear equations:

$$\sum_{j=1}^{2}(C_{ij} - \lambda G_{ij})V_j = 0,\ i = 1,2, \tag{24}$$

being $G_{ij} = \widehat{\mathbf{E}}_i \cdot \widehat{\mathbf{E}}_j = \delta_{ij}$, the elements of the Gram's matrix associated with the vector basis E. The possible values of λ are the solutions of the characteristic equation:

$$\begin{vmatrix} C_{11}-\lambda & C_{12} \\ C_{21} & C_{22}-\lambda \end{vmatrix} = 0, \tag{25}$$

$$\lambda_1 = t + \sqrt{t^2 - I_2},\ \lambda_2 = t - \sqrt{t^2 - I_2}, \tag{26}$$

with

$$t = \frac{I_1}{2} = \frac{1}{2}(C_{11} + C_{22}),\ I_2 = C_{11}C_{22} - C_{12}^2. \tag{27}$$

Both solutions are real and positive because $I_2 > 0$, $t > 0$ and $t^2 - I_2 > 0$. Furthermore $\lambda_1 > \lambda_2$. The latter are known as the principal quadratic elongations (Ramsay, 1967, p. 65).

In order to characterize the *intensity of the strain* by a single number, we use the strain ratio (Ramsay, 1967, p. 199):

$$R = \frac{\sqrt{\lambda_1}}{\sqrt{\lambda_2}}, \tag{28}$$

the ratio of the lengths of the major and minor semi-axes of the strain ellipse. Finally, using Eq. (26), we obtain:

$$R = z + \sqrt{z^2 - 1}, \tag{29}$$

with

$$z = \frac{t}{\sqrt{I_2}} = \frac{(1 - \kappa(X)d(X,Y))^2 + d_1(X,Y)^2 + d_2(X,Y)^2}{2(1 - \kappa(X)d(X,Y))d_2(X,Y)}. \tag{30}$$

7. Particular cases of tangential longitudinal strain (TLS)

Taking into account the descriptions of folding by TLS found in the geological literature, two different models of this mechanism will be considered.

7.1. Parallel tangential longitudinal strain (PTLS)

In this model, the orthogonal thickness of the bed is kept constant and the strain ellipse axes remain tangential and normal to the layer boundaries during folding. Consequently, the area varies heterogeneously throughout the folded layer. According to this, the neutral line separates an inner arc with $\lambda_1 = 1$ from an outer arc $\lambda_2 = 1$.

7.2. Equiareal tangential longitudinal strain (ETLS)

In this model, the folding deformation maintains constant area throughout the folded layer, and produces a thickening of the inner arc and a thinning of the outer arc. In the general case with variation of curvature along the neutral line, this model gives rise to obliquity between the strain ellipse axes and the layer boundaries (Bobillo-Ares et al., 2000).

These two models represent extreme scenarios that can be combined to simulate intermediate situations.

8. Parallel tangential longitudinal strain (PTLS)

In this folding mechanism, the distance from any particle to the neutral line remains constant during the folding process. The mechanism is characterized by the straightforward condition:

$$d(X,Y) = Y, \tag{31}$$

$$d_1(X,Y) = 0, \; d_2(X,Y) = 1. \tag{32}$$

The corresponding area ratio is obtained by substituting these expressions in Eq. (17):

$$J(X,Y) = 1 - \kappa(X)Y. \tag{33}$$

On the other hand, from Eqs. (21)–(23) we have:

$$C_{11} = (1 + \kappa(X)Y)^2, \; C_{22} = 1, \; C_{12} = 0. \tag{34}$$

As $[C_{ij}]$ is a diagonal matrix, the principal directions are those of vectors $\widehat{\mathbf{E}}_1$ and $\widehat{\mathbf{E}}_2$, and the corresponding principal values are C_{11} and C_{22}, which, ordered from higher to lower values, give:

$$\lambda_1 = \begin{cases} 1 & Y > 0 \\ (1 - \kappa(X)Y)^2 & Y < 0 \end{cases} \tag{35}$$

$$\lambda_2 = \begin{cases} (1 - \kappa(X)Y)^2 & Y > 0 \\ 1 & Y < 0 \end{cases}. \tag{36}$$

Hence,

$$R = 1 - \kappa(X)Y \;\; \text{(for the outer arc)}, \tag{37}$$

$$R = \frac{1}{1 - \kappa(X)Y} \;\; \text{(for the inner arc)}. \tag{38}$$

These equations are represented graphically in Fig. 2 for several Y values.

Moreover, from Eqs. (33), (35) and (36), we have:

$$J = R \;\; \text{(for the outer arc)}, \tag{39}$$

$$J = \frac{1}{R} \;\; \text{(for the inner arc)}. \tag{40}$$

If area change is expressed as a dilation ($\Delta = J - 1$), we have:

$$\Delta = \kappa(X)Y \;\; \text{(for the outer arc)}, \tag{41}$$

$$\Delta = -\kappa(X)Y \;\; \text{(for the inner arc)}. \tag{42}$$

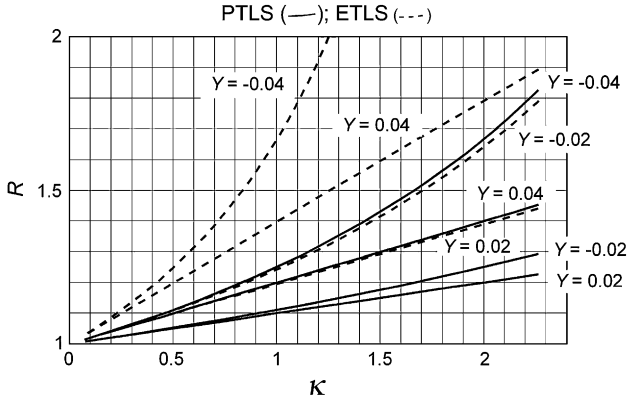

Fig. 2. Variation of R as a function of the curvature κ of the neutral line for PTLS and ETLS (dashed lines).

This result indicates that the percentage area decrease at point (X, Y) equals the percentage area increase at point $(X, -Y)$.

PTLS is a mechanism that could be ideally expected during folding of a highly compressible material. A visualization of this mechanism is given by the hypothetical folding of a flexible comb with convergent teeth that simulate the layer normals. In reality, a deforming rock would resist such area changes and this will hamper the operation of this ideal folding mechanism.

9. Equiareal tangential longitudinal strain (ETLS)

In this case, the folding mechanism is completely defined by adding the condition of area conservation (incompressibility condition): $J(X, Y) = 1$. That is:

$$(1 - \kappa(X)d(X,Y))d_2(X,Y) = 1. \tag{43}$$

This simple partial differential equation can be directly integrated (Bobillo-Ares et al., 2000) to obtain the equation:

$$\kappa(X)d(X,Y)^2 - 2d(X,Y) + 2Y = 0, \tag{44}$$

and from here:

$$d(X,Y) = \frac{1 - \sqrt{1 - 2Y\kappa(X)}}{\kappa(X)}. \tag{45}$$

The positive sign of the root must be rejected since it would lead to a negative area ratio.

Finally, note that ETLS is only meaningful when the radicand in Eq. (45) is positive, i.e., when the following condition holds:

$$Y < \frac{\rho}{2}. \tag{46}$$

Application of Eqs. (21)–(23) and (26) allows the principal values of strain and the strain ratio R to be obtained, though a short analytical expression cannot be derived for them in this case. Fig. 2 shows the variation of R as a function of the curvature for several Y values and allows comparison of the curves obtained for ETLS and PTLS. Since R slightly depends on the derivative of the curvature (Bobillo-Ares et al., 2000), very small variations can be expected in these curves depending on the function that represents the final form of the neutral line.

10. Mathematical modelling of folds formed by tangential longitudinal strain: comparison of results

Folds formed by tangential longitudinal strain can be modelled using the program "FoldModeler", developed in the MATHEMATICA™ environment (Bobillo-Ares et al., 2004), by application of successive folding steps to an original configuration of the layer profile defined by a grid of small quadrilaterals. The nodes of the grid are transformed according to the relationships defined for the two types of tangential longitudinal strain, and this permits the folded layer configuration and strain state to be obtained. The initial neutral line has been located midway to the layer boundaries, though FoldModeler allows it to be placed also in non-central positions. The program allows the application of any combination of the two variants of TLS described, by superposition of individual folding steps. Each folding step is defined by specifying the type of mechanism to be applied, the increment that it produces in the normalised amplitude of the fold (height/width ratio for the fold limb ($h = y_0/x_0$), measured on the neutral line; Fig. 3), and the form of the neutral line, that is defined by a piece of a conic section characterised by its eccentricity (e) (Aller et al., 2004); this parameter can be chosen freely and in this paper the parabolic form ($e = 1$) has been used as a simple form that fits the shape of many natural folds. The superposition of mechanisms can be successive or simultaneous; the latter requires addition of a large number of very low amplitude alternating folding steps of ETLS and PTLS. The new version of "FoldModeler" used here introduces the new mechanism PTLS (ETLS was operative in previous versions), and allows the simultaneous modelling of both fold limbs, though folds generated in this paper are always symmetric.

Curves that show the variation of R, J and ϕ (the angle of inclination of the major axis of the strain ellipse) along the inner and the outer arc, as a function of the layer dip α, have been used to analyse the strain distribution in the folded layer (Figs. 4–8). Fig. 3 shows the sign convention for angles ϕ and α. The curves

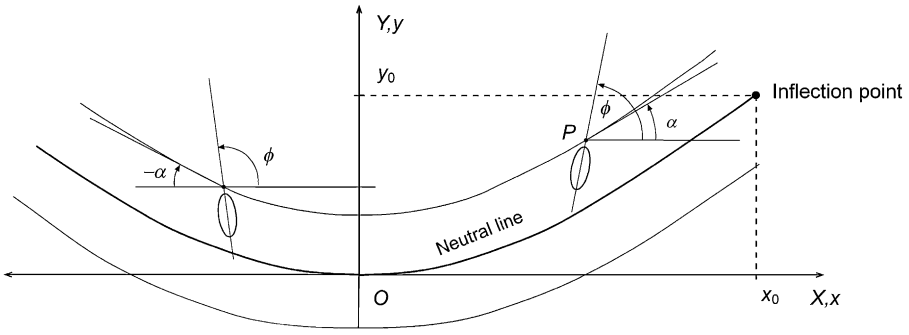

Fig. 3. Elements to define the normalised amplitude ($h = y_0/x_0$) of the folded layer and the angles used to study the strain distribution. α is the dip of the layer at P and ϕ defines the plunge of the major axis of the strain ellipse at that point.

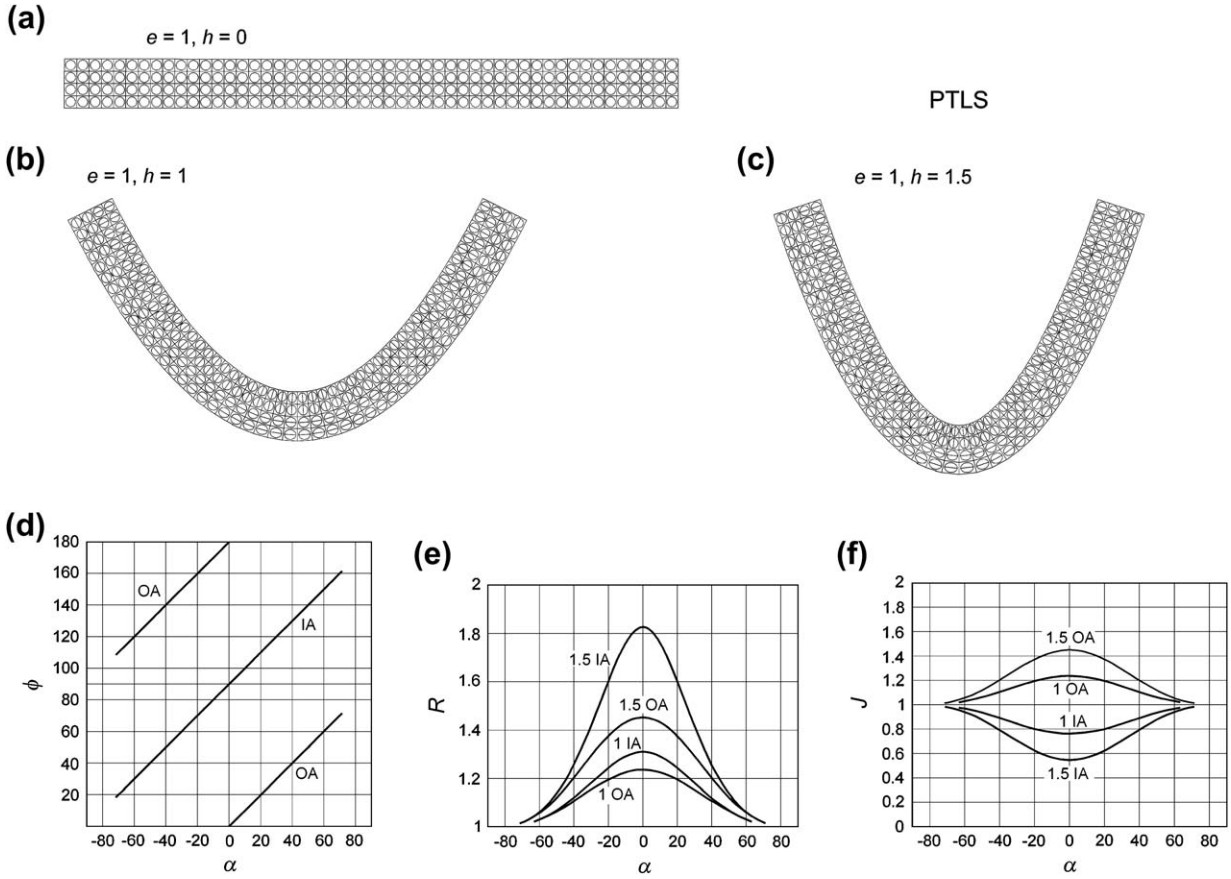

Fig. 4. Graphical results for parallel tangential longitudinal strain folding (PTLS). (a), (b) and (c) Initial and folded configuration of the folded layer for normalised amplitudes 1 and 1.5. (d), (e) and (f) Variation of ϕ (inclination of the major axis of the strain ellipse), R (axial ratio of the strain ellipse), and J (area ratio) as a function of the layer dip α. IA, inner arc; OA, outer arc.

have been obtained for an original layer with 40 rows and 500 columns, folded to normalised amplitudes of 1 and 1.5. Nevertheless, to allow a better visualization of the folded layer, this is shown in Figs. 4–8 with only four rows and 50 columns. For the folded layer with a normalised amplitude of 1.5, other curves have also been obtained that show the variation of the maximum R and J values for the inner and the outer arc, as a function of the percentage of PTLS and ETLS taking part in a successive or simultaneous superposition of the two mechanisms (Fig. 9).

10.1. Modelling of the individual PTLS and ETLS

Results for the modelling of pure PTLS and ETLS are shown in Figs. 4 and 5. In both cases, the major axes of the strain ellipse show a convergent fan in the inner arc and a concentric or nearly concentric pattern in the outer arc. Nevertheless, important differences are observed between both types of TLS that can be summarised in the following points:

- The ϕ vs. α curves show linear patterns for PTLS, whereas for ETLS a deviation from linearity exists, mainly in the inner arc, in which the function ϕ is multivalued for the amplitude of 1.5. Discontinuities observed in the outer arc curves at $\alpha = 0$ are due to the variation of ϕ from 0 to 180° in the hinge point.
- In the R vs. α curves (Figs. 4 and 5) and the R vs. κ curves (Fig. 2), maximum R values are found in the hinge point, and are higher for ETLS (9.53 in the inner arc and 1.89 in the outer arc for $h = 1.5$) than for PTLS (1.83 and 1.45, respectively). Moreover, the R vs. α curve for the inner arc with $h = 1.5$ shows a loop in the α interval (−30, 30).
- The multivalued character of the inner arc R and ϕ functions for ETLS with $h = 1.5$ is related with the development of a bulge near the hinge zone of the corresponding fold. The increase of normalised amplitude gives rise to high curvature and curvature variation values in the hinge zone that increase the tangential shortening in the inner arc and produce the bulge. This does not appear in PTLS folding.
- In PTLS, extreme area variations are found at the hinge points. For $h = 1.5$, $J = 0.55$ in the inner arc (45% area decrease) and 1.45 in the outer arc (45% area increase). As observed, the absolute value of the percentage is equal in both arcs. In ETLS, no area change occurs in theory; nevertheless, in the inner arc of the hinge zone, small area change values are observed (Fig. 9), due to the discrete character of the division of the folded layer in quadrilaterals.

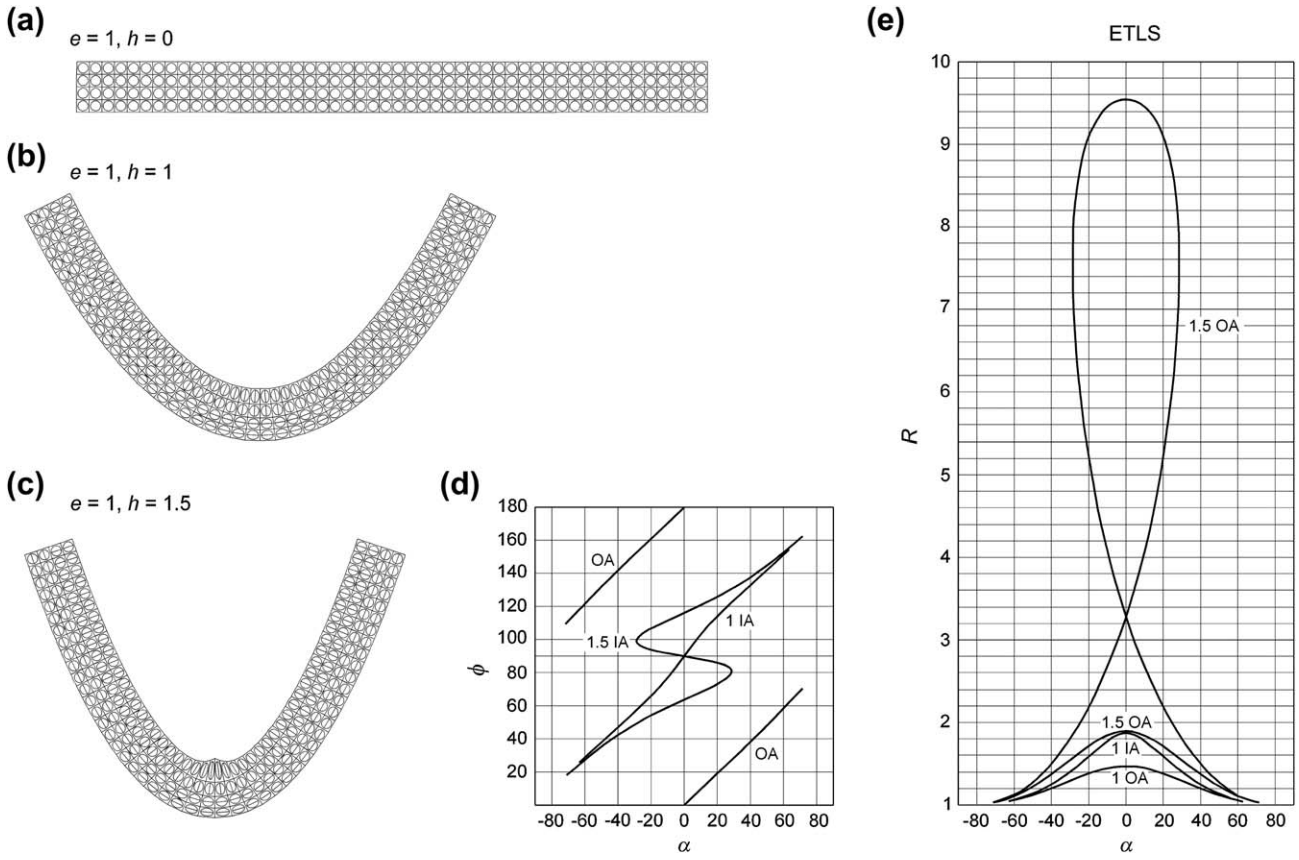

Fig. 5. Graphical results for equiareal tangential longitudinal strain folding (ETLS). (a), (b) and (c) Initial and folded configuration of the folded layer for normalised amplitudes 1 and 1.5. (d) and (e) Variation of ϕ and R as a function of the layer dip α. IA, inner arc; OA, outer arc.

10.2. Successive superposition of PTLS and ETLS

For the study of folds formed by ETLS followed by PTLS or vice versa, each mechanism was applied to produce one half of the final amplitude.

With a sequence ETLS–PTLS (Fig. 6), some features resemble those obtained with PTLS as a single mechanism (Fig. 4), e.g. no bulge is formed and the $\phi - \alpha$ curves show a nearly linear pattern. Nevertheless, maximum R values are higher (2.37 in the inner arc and 1.62 in the outer arc for $h = 1.5$), and area change values lower (39% decrease in the inner arc and 24% increase in the outer arc) than for pure PTLS. An important difference with the pure PTLS folding is that in the ETLS–PTLS sequence the percentage of area decrease in the inner arc (39%) is higher than the percentage of area increase in the outer arc (24%). This difference is produced because when PTLS begins to operate, the neutral line, as a result of the ETLS stage, is not equidistant from the layer boundaries, since the inner arc is thicker than the outer arc. Thus, the percentage of inner arc shortening during the PTLS stage is higher than the percentage of outer arc stretching.

Some results of the PTLS–ETLS sequence (Fig. 7) resemble those obtained with pure ETLS, e.g. a bulge, though smaller, appears for $h = 1.5$, the $\phi - \alpha$ curves are nonlinear for the inner arc, and loops appear in the $R - \alpha$ and $J - \alpha$ curves of this arc. R maximum values are lower than in pure ETLS (4.86 in the inner arc and 1.70 in the outer arc for $h = 1.5$). As in pure PTLS, area change percentages should be the same in both arcs. Nevertheless, the values observed ($J = 0.80$ or 20% area reduction in the inner arc, and $J = 1.16$ or 16% area increase in the outer arc for $h = 1.5$) show a difference of 4% that can be explained by the high R values and the discrete division of the folded layer in quadrilaterals. The results presented above indicate that the successive superposition of the two mechanisms gives rise to folds with characteristics intermediate between those of the folds obtained with pure ETLS and PTLS.

It is probable that a combination of both mechanisms in natural folding begins with ETLS in the first stages, when the amplitude, curvature and curvature variation of the neutral line are low. When the amplitude increases, the curvature and the curvature variation generally concentrate in the hinge zone. Thus, high strain values appear in this zone, and it is more and more difficult to preserve area constant there. This is the stage when PTLS becomes probable. It makes possible area change and prevents the development of a bulge in the inner arc. The final result of the superposition is a fold with features intermediate between those of pure ETLS and PTLS. These pure mechanisms appear as extreme possibilities spanning an infinite number of intermediate combinations.

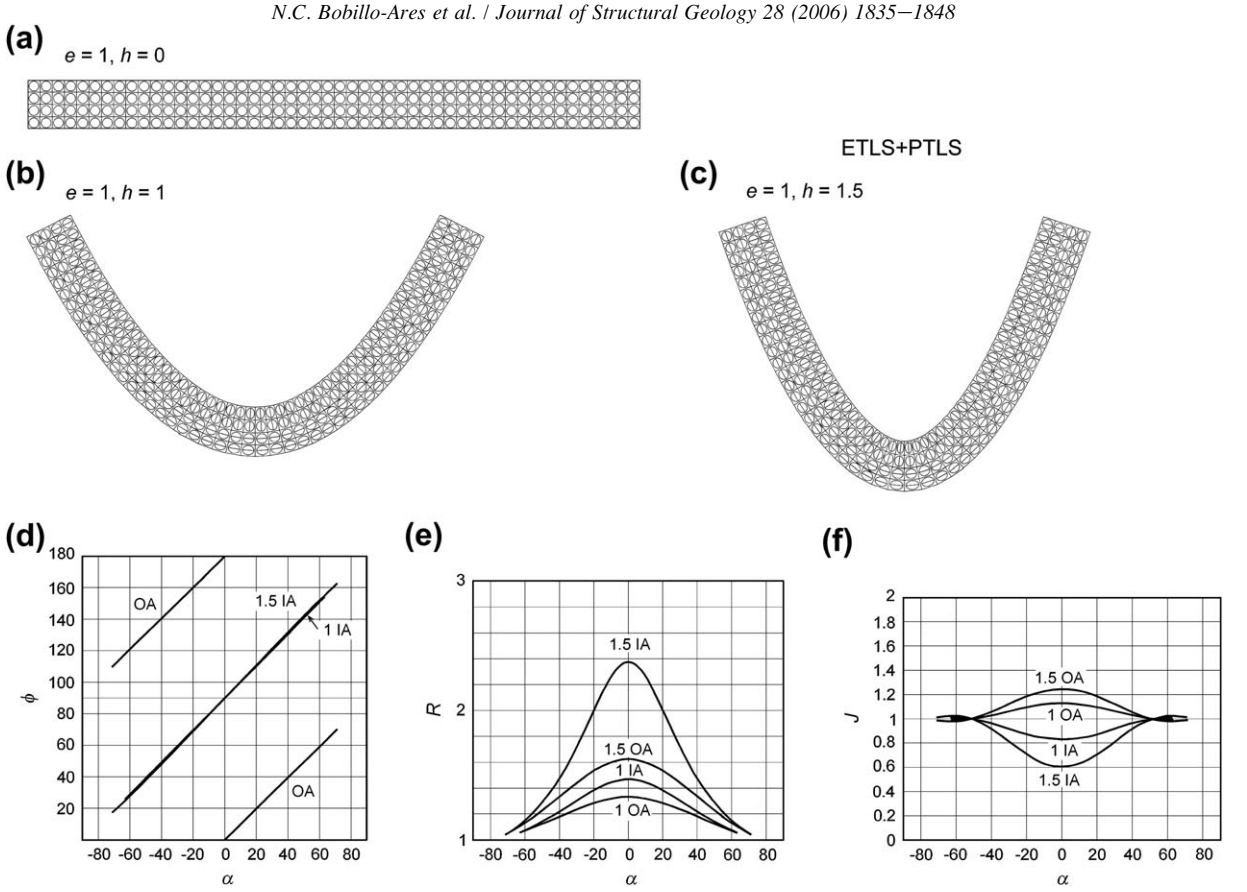

Fig. 6. Graphical results for the ETLS–PTLS folding sequence. Each mechanism is responsible for one half of the final amplitude. (a), (b) and (c) Initial and folded configuration for normalised amplitudes 1 and 1.5. (d), (e) and (f) Variation of ϕ, R, and J as a function of the layer dip α. IA, inner arc; OA, outer arc.

10.3. Simultaneous superposition of PTLS and ETLS

The results obtained in this case (Fig. 8) are characterised by ϕ, R and J values which are in general intermediate between those obtained both for the sequences ETLS–PTLS and PTLS–ETLS. With $h = 1.5$, there is no bulge in the hinge zone, but the $\phi - \alpha$ curve is not linear for the inner arc of the folded layer. R values are also intermediate between those found in the sequences cited (3.11 in the inner arc and 1.66 in the outer arc for $h = 1.5$), and the same happens with the area change ($J = 0.68$ in the inner arc and $J = 1.2$ in the outer arc for $h = 1.5$).

10.4. Generalised superposition of PTLS and ETLS

To analyse the effects of the successive or simultaneous superposition of the two types of TLS with variable intensity, some curves have been obtained that show the variation of R and J in the hinge point of the inner and the outer arc against the percentage of each type of TLS (Fig. 9). This percentage is measured from the ratio between the normalised amplitude reached by the mechanism considered and the total amplitude of the fold that results from the superposition. From these curves the following conclusions are drawn:

- The intensity of strain (R value) is always higher in the inner arc than in the outer arc for any combination of ETLS and PTLS. Nevertheless, the difference in intensity between the two arcs decreases as the percentage of PTLS increases.
- R always decreases as the percentage of PTLS increases. The decrease is much more intense in the inner than in the outer arc.
- In the inner arc, the curves are very different depending on the superposition order. For the sequence ETLS–PTLS, the decrease in R is quite abrupt for small percentages of PTLS, and then it is less pronounced. On the other hand, for the sequence PTLS–ETLS, decrease in R is quite constant, nearly linear, as the percentage of PTLS increases. With simultaneous superposition of both mechanisms, results are intermediate between those found in the previous sequences.
- In the outer arc, the form in the R curves depends only slightly on the superposition order.
- Area change (J) curves always show an increase in the outer arc and a decrease in the inner arc as the percentage of PTLS increases.
- J curves for the inner arc are different depending on the order of application of the mechanisms. J variation is more abrupt for small percentages of PTLS in the sequence ETLS–PTLS than in PTLS–ETLS, with an intermediate situation in the case of simultaneous superposition. The variations in the outer arc for the different sequences are small.

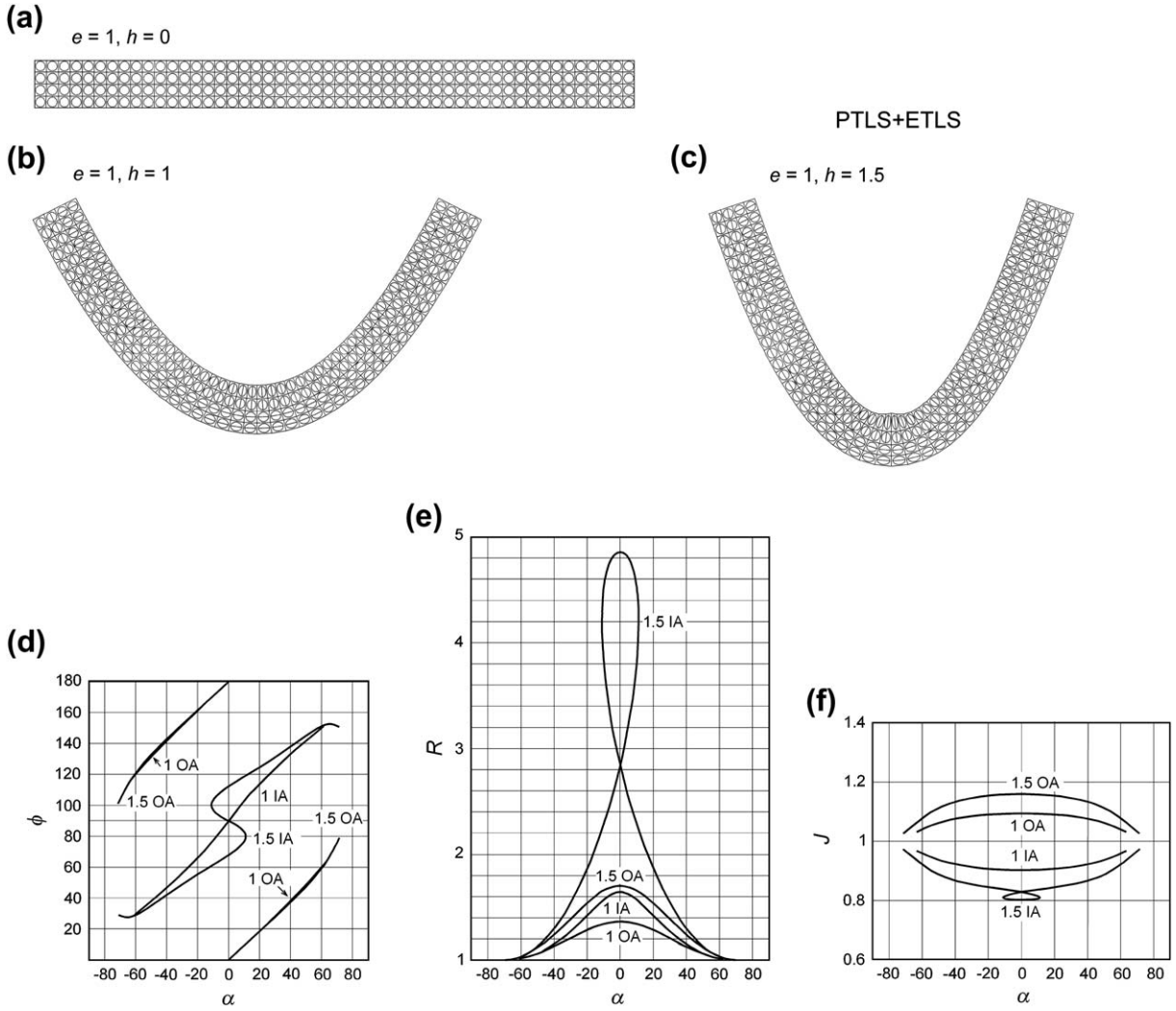

Fig. 7. Graphical results for the PTLS–ETLS folding sequence. Each mechanism is responsible for one half of the final amplitude. (a), (b) and (c) Initial and folded configuration for normalised amplitudes 1 and 1.5. (d), (e) and (f) Variation of ϕ, R, and J as a function of the layer dip α. IA, inner arc; OA, outer arc.

11. Tangential longitudinal strain in natural folds

Some structures common in the hinge zone of folds at the outcrop scale have been attributed to TLS. The presence of a bulge in the inner arc of the hinge zone clearly indicates that ETLS played an important role in the formation of the fold (Fig. 10a). In other cases, the intense deformation in the inner arc is accommodated through the development of reverse faults that suggest brittle accommodation of a bulge related to ETLS (Fig. 10b).

The presence of wedge-shaped radial veins increasing in thickness towards the outer arc of the hinge zone and filled with minerals as quartz or calcite, indicates tangential stretching of the outer arc and area creation on the fold profile by fracturing (Fig. 11). These structures are a manifestation of TLS folding through a brittle deformation whose ductile equivalent can be considered PTLS. Similarly, the presence of a convergent cleavage, mainly formed by pressure solution, in the inner arc of the hinge zone suggests elimination of material and area reduction, which can also be related to PTLS activity. Ormand and Hudleston (2003) suggested that the material that is eliminated from the inner arc of the hinge zone can crystallise then in veins or cracks.

Radial cracks in the outer arc of the hinge zone and convergent cleavage in the inner arc are quite common in natural folds. However, structures ''a priori'' complementary to these, such as concentric cleavage in the outer arc or concentric extensional veins in the inner arc are very rare. The lack of concentric cleavage in the outer arc can be explained because the intensity of strain is usually low in this arc (Figs. 4–8), but the lack of concentric extensional veins in the inner arc poses a paradox if folding is explained as a result of ETLS, which produces high R values in the inner arc. In fact, in brittle–ductile shear zones, probably developed in conditions similar to those of TLS, tension cracks are much more common than cleavage. A possible explanation is that the lack of concentric extensional veins is due to the operation of the PTLS mechanism, which involves lower R values and the absence of stretching in the direction of the major axis of the strain ellipse in the inner arc of the hinge zone.

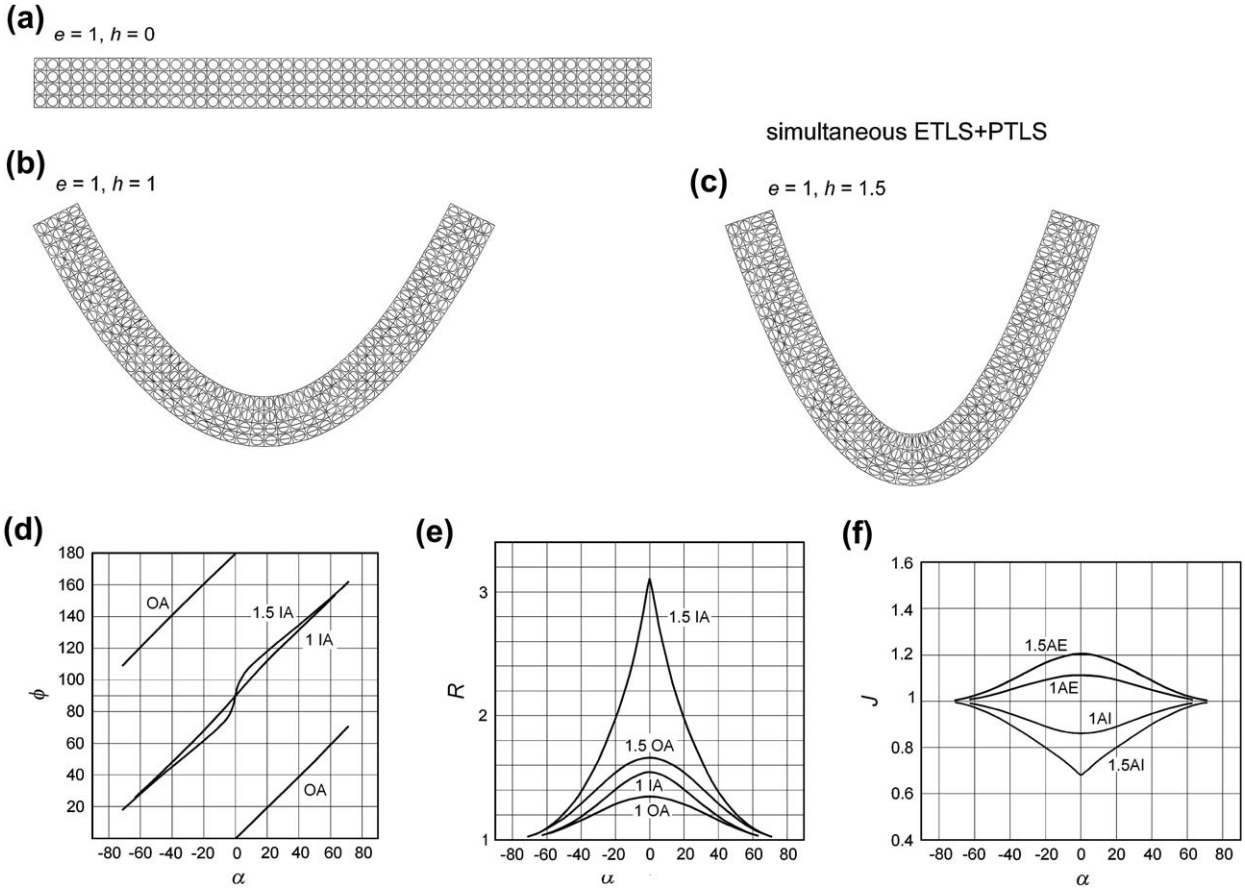

Fig. 8. Graphical results for the folding sequence with simultaneous superposition of PTLS–ETLS, simulated by the application of an alternation of small amplitude PTLS and ETLS folding steps. Each mechanism is responsible for one half of the final amplitude. (a), (b) and (c) Initial and folded configuration for normalised amplitudes 1 and 1.5. (d), (e) and (f) Variation of ϕ, R, and J as a function of the layer dip α. IA, inner arc; OA, outer arc.

12. Discussion and conclusions

The analysis of the kinematical mechanisms operating in natural folds has brought to light that TLS, with all its variants, is a very common mechanism in the buckling of individual competent layers (Ramsay, 1967; Hudleston and Holst, 1984; Ramsay and Huber, 1987; Hudleston and Tabor, 1988; Lemiszki et al., 1994; Hudleston and Srivastava, 1997; Gutiérrez-Alonso and Gross, 1999; Ormand and Hudleston, 2003; Toimil, 2005). Nevertheless, a consistent definition of this mechanism is necessary, since in some cases two simultaneous properties have been attributed to folds formed by TLS that in general are mutually incompatible: the maintaining of the principal directions of strain tangential and normal to the layer boundaries, and area conservation in the fold layer profile. On the other hand, some authors, taking into account structures commonly associated with folds, have proposed models of tangential longitudinal strain with area change (Hudleston and Holst, 1984; Hudleston and Tabor, 1988; Hudleston and Srivastava, 1997; Ormand and Hudleston, 2003). Nevertheless, the properties of these models have not yet been developed from a theoretical point of view.

This paper presents the mathematical development of a general model of TLS based on two simple conditions: a neutral line exists, and straight lines originally normal to the neutral line remain straight and normal to it as folding progresses. From this general model, two particular cases have been developed and analysed. The first of them, named parallel tangential longitudinal strain (PTLS), implies conservation of the bed orthogonal thickness (parallel folds), so that the original distance from the neutral line to the layer boundaries is maintained constant during folding. In this model, one of the principal values of strain is the unit (λ_1 in the inner arc and λ_2 in the outer arc) and the corresponding principal direction is normal to the layer boundaries, whereas the other principal direction is a tangential stretching in the outer arc (λ_1) and a tangential shortening in the inner arc (λ_2), whose value in both cases is $(1-\kappa(X)Y)^2$; the area on the layer profile changes as deformation progresses in a way that the percentage of area decrease in the inner arc for an initial point (X, Y) equals the percentage of area increase in the initial point $(X, -Y)$. The second case studied is the equiareal tangential longitudinal strain (ETLS), already studied by Bobillo-Ares et al. (2000).

Some authors have proposed mechanisms that can be considered special types of PTLS, e.g. the ‘‘inner arc collapse by volume loss’’ (Hudleston and Holst, 1984; Hudleston and Tabor, 1988) or the ‘‘outer arc stretching’’ (Ormand and

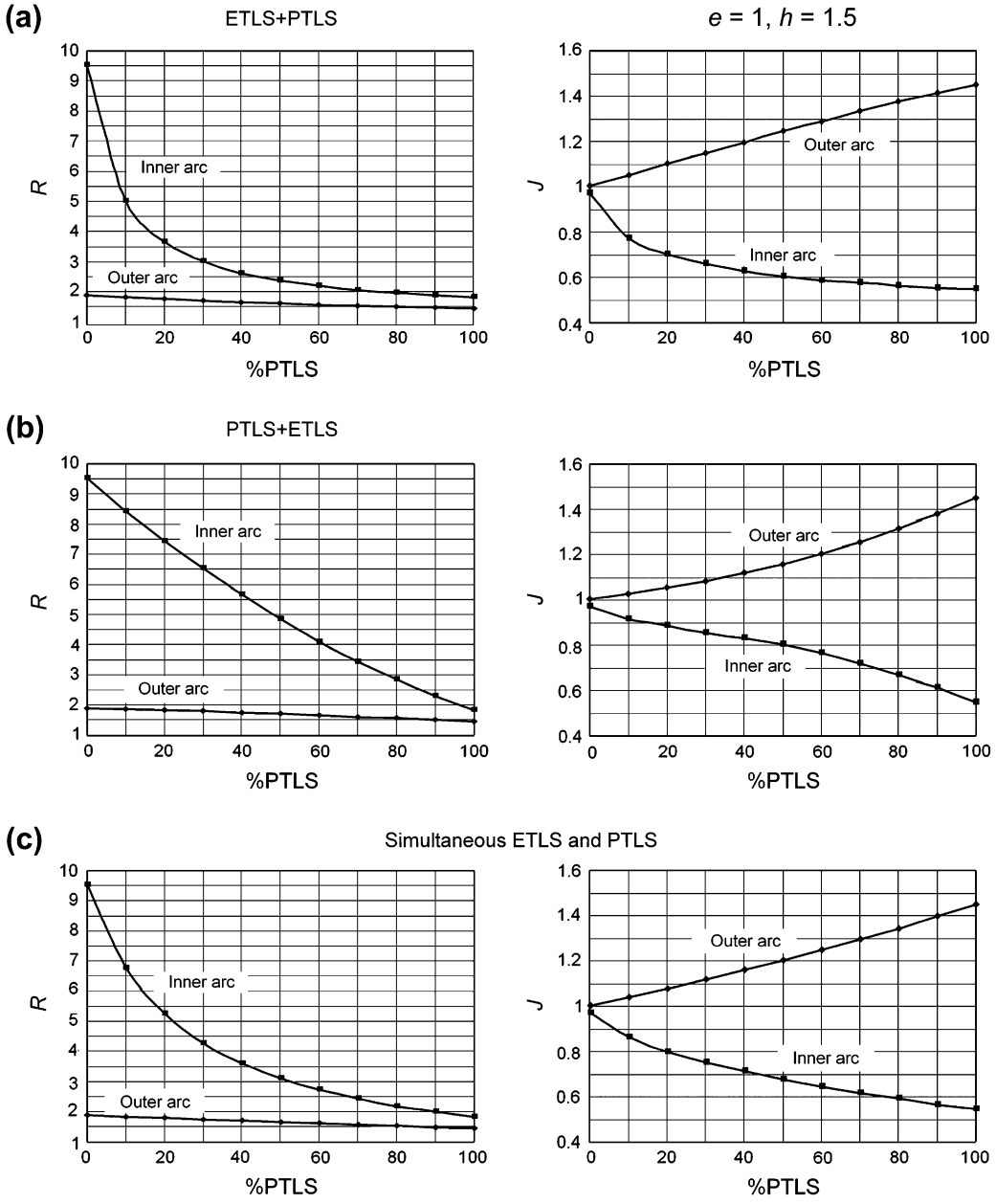

Fig. 9. Generalised superposition of PTLS and ETLS. (a) Results when ETLS is applied before. (b) Results when PTLS is applied before. (c) Results for simultaneous application of PTLS and ETLS.

Hudleston, 2003). These mechanisms can be considered to be particular cases of PTLS with a different location of the neutral line, which in the first case is located in the outer arc, and in the second in the inner arc.

Computer modelling of PTLS and ETLS folds using the program "FoldModeler" (Bobillo-Ares et al., 2004) has shed light on the geometrical properties of folds formed by these two mechanisms and by the successive or simultaneous combination of them. Comparing pure PTLS and ETLS folds, it is observed that maximum R values are found in the hinge point and are higher for ETLS than for PTLS. Moreover, in the hinge zone, the evolution of folding produces in many cases an increase in the curvature variation. This gives rise to intense local R variations in the inner arc that locally thicken the bed to form bulges for ETLS folding.

Successive or simultaneous superposition of PTLS and ETLS gives rise to folds with characteristics intermediate between those of the pure mechanisms, which appear as extreme cases separating an infinite range of possibilities. On the other hand, in cases with successive superposition, results are quite different, mainly for the inner arc, depending on the order of the mechanisms. It is suggested that in natural folds it is probable that TLS deformation begin with ETLS. PTLS becomes important as deformation increases, mainly in the inner arc, and its accommodation without area change is difficult.

Geometrical models such as those analysed here allow predictions about the minor structures that can develop in

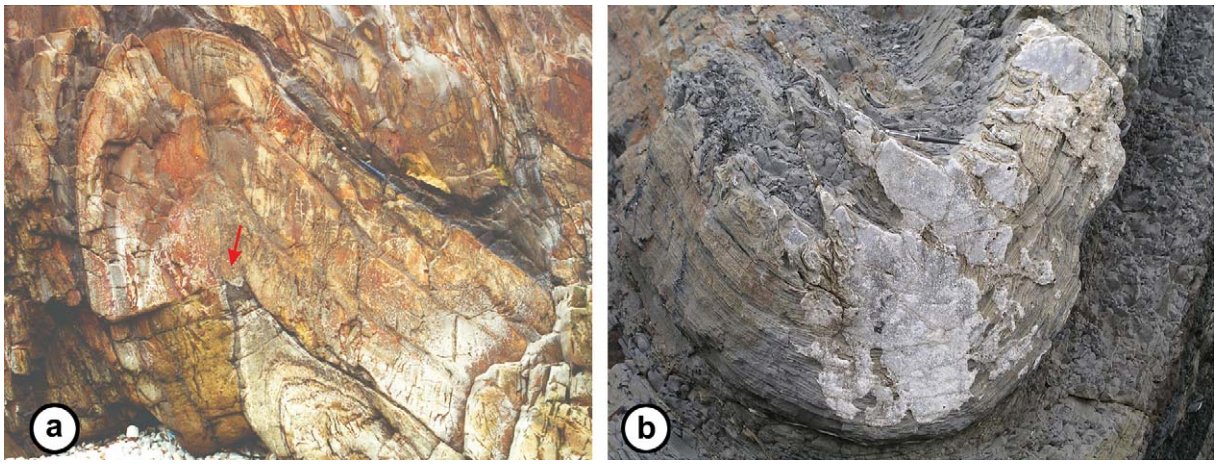

Fig. 10. (a) Development of a bulge in the inner arc of a fold formed by TLS in Cambro-Ordovician sandstones near Tapia de Casariego (Asturias, Spain). Bed thickness is greater in the hinge zone than on the limbs because of post-TLS flattening. (b) Development of reverse faults in the inner arc of a syncline in Cretaceous turbidities of the Barrika beach (Biscay, Spain).

different parts of the folded layer. Conversely, structures observed in natural folds can be interpreted as a result of the operation of a specific mechanism. Thus, minor structures common in the hinge zone of natural folds are indicative of the different types of TLS. The presence of a bulge or reverse faults in the inner arc is related to ETLS, whereas wedge-shaped mineralized cracks opening towards the outer arc or pressure solution cleavage in the inner arc are related to PTLS. The lack of concentric cracks in the inner arc near the hinge zone suggests an important contribution of PTLS.

Fig. 11. Development of wedge-shaped quartz veins opening towards the outer arc in the hinge zone of competent layers (Carboniferous flysch, Santo Toribio de Liébana, Cantabria, Spain).

A quantitative precise discrimination of the TLS mechanisms involved in natural folds is difficult at present using theoretical models, due to the difficulty to determine the strain at points of the folded layer. The presence of cleavage gives an approach to the distribution of the strain principal directions, but this structure is not probable in folds formed only by TLS. Nevertheless, when TLS is associated with homogeneous strain (e.g. layer shortening or fold flattening) development of cleavage is probable, and it can be used to obtain a quantitative approach to the involved folding mechanisms by the method described by Bastida et al. (2003).

Ramsay (1967, p. 401) and Ramsay and Huber (1987, p. 460–461) proposed the mechanism of "neutral line migration" to mitigate the space problem that appears in the inner arc of ETLS folds with high strain values. In this mechanism, the neutral line changes its material location during folding and moves towards the inner arc. Modelling this process is difficult, but a good approximation to the resulting folded configuration that it produces can be obtained with the program "FoldModeler", assuming that the neutral line is not located midway between the layer boundaries in the original configuration, but it is located nearer to the boundary that will become inner arc.

According to Ramsay (1967, p. 400), another way to avoid the high strain concentrations in the inner arc is to increase the curvature of the limbs and to maintain hinge curvature constant as folding progresses. This would lead to a tendency for rounded fold profile shapes. Nevertheless, if the curvature increases in the fold inflection points, a problem arises in connecting successive folds, since there would exist a deformation discontinuity in these inflection points both for ETLS and PTLS. This makes a curvature increase near the inflection points improbable. Another possibility to avoid the high strain concentrations in the inner arc is that the folding mechanism changes, e.g. to flexural flow (Ramsay, 1967, pp. 400–401).

Hinge migration during folding has been described by several authors (e.g. Fowler and Windsor, 1996; Ghosh et al., 1996; Zhang et al., 2000) and it is probable to occur in

some cases during TLS. Geometrical modelling of this migration is difficult. Nevertheless, it can explain the presence of features typical of the hinge zone (e.g. wedge-shaped veins in the outer arc) outside the final hinge zone.

Although TLS models analysed here are all 2D, the results obtained allow some suggestions about the 3D geometry of the folds. Thus, assuming isochoric deformation, which is reasonable in competent rocks suffering TLS, anticlastic bending (Ferguson and Andrews, 1928; Ramsay, 1967, p. 402) and possible related features would be related to PTLS.

Acknowledgements

The present work has been supported by Spanish CGL2005-02233-BTE project of the Spanish Ministerio de Ciencia y Tecnología and Fondo Europeo de Desarrollo Regional (FEDER). We are grateful to Jordi Carreras and Deepak Srivastava for many valuable suggestions.

Appendix A. Important definitions

The notation $B = A + \mathbf{v}$ indicates that B is the point that results from translating point A by vector $\mathbf{v}$. This implies that $A + \overrightarrow{AB} = B$. In order to define derivatives of point functions, it is convenient to introduce the difference of points as a vector:

$$B - A := \overrightarrow{AB}. \tag{A1}$$

The oriented area of a parallelogram characterized by the ordered pair of vectors $\mathbf{a}$ and $\mathbf{b}$ is designed by $S(\mathbf{a}, \mathbf{b})$. In any arbitrary basis $e = (\mathbf{e}_1, \mathbf{e}_2)$ in the plane we have, by the bilinearity and alternance properties of $S(\cdot, \cdot)$:

$$S(\mathbf{a}, \mathbf{b}) = \begin{vmatrix} a_1 & b_1 \\ a_2 & b_2 \end{vmatrix} S(\mathbf{e}_1, \mathbf{e}_2), \tag{A2}$$

being $\mathbf{a} = a_1\mathbf{e}_1 + a_2\mathbf{e}_2$ and $\mathbf{b} = b_1\mathbf{e}_1 + b_2\mathbf{e}_2$. By convention, if e is a direct orthonormal basis, we put: $S(\mathbf{e}_1, \mathbf{e}_2) = +1$.

References

Aller, J., Bastida, F., Toimil, N.C., Bobillo-Ares, N.C., 2004. The use of conic sections for the geometrical analysis of folded surface profiles. Tectonophysics 379, 239–254.

Bastida, F., Bobillo-Ares, N.C., Aller, J., Toimil, N.C., 2003. Analysis of folding by superposition of strain patterns. Journal of Structural Geology 25, 1121–1139.

Bobillo-Ares, N.C., Bastida, F., Aller, J., 2000. On tangential longitudinal strain folding. Tectonophysics 319, 53–68.

Bobillo-Ares, N.C., Toimil, N.C., Aller, J., Bastida, F., 2004. FoldModeler: a tool for the geometrical and kinematical analysis of folds. Computers & Geosciences 30, 147–159.

Ferguson, A., Andrews, J.P., 1928. An experimental study of the anticlastic bending of rectangular bars of different cross sections. Proceedings of the Physical Society 41, 1–17.

Fowler, T.J., Windsor, C.N., 1996. Evolution of chevron folds by profile shape changes: comparison between multilayer deformation experiments and folds of the Bendigo–Castlemaine gold fields, Australia. Tectonophysics 258, 125–150.

Ghosh, S.K., Deb, S.K., Sengupta, S., 1996. Hinge migration and hinge replacement. Tectonophysics 263, 319–337.

Gutiérrez-Alonso, G., Gross, M.R., 1999. Structures and mechanisms associated with development of a fold in the Cantabrian Zone thrust belt, NW Spain. Journal of Structural Geology 21, 653–670.

Hudleston, P.J., Holst, T.B., 1984. Strain analysis and fold shape in a limestone layer and implication for layer rheology. Tectonophysics 106, 321–347.

Hudleston, P.J., Srivastava, H.B., 1997. Strain and crystallographic fabric pattern in a folded calcite vein: the dependence on initial fabric. In: Sengupta (Ed.), Evolution of Geological Structures in Micro- to Macro-scales. Chapman & Hall, London, pp. 259–271.

Hudleston, P.J., Tabor, J., 1988. Strain and fabric development in a buckled calcite vein and rheological implications. Bulletin of the Geological Institutions of the University of Uppsala 14, 79–94.

Hudleston, P.J., Treagus, S.H., Lan, L., 1996. Flexural flow folding: does it occur in nature? Geology 24, 203–206.

Kuenen, P.U., de Sitter, L.U., 1938. Experimental investigation into the mechanism of folding. Leidse Geologische Mededelingen 10, 217–240.

Lemiszki, P.J., Landes, J.D., Hatcher Jr., R.D., 1994. Controls on hinge-parallel extension fracturing in single-layer tangential–longitudinal strain folds. Journal of Geophysical Research 99, 22,027–22,041.

Ormand, C.J., Hudleston, P.J., 2003. Strain paths of three small folds from the Appalachian Valley and Ridge, Maryland. Journal of Structural Geology 25, 1841–1854.

Ramberg, H., 1961. Relationships between concentric longitudinal strain and concentric shearing strain during folding of homogeneous sheets of rock. American Journal of Science 259, 382–390.

Ramsay, J.G., 1967. Folding and Fracturing of Rocks. McGraw-Hill Book Comp., New York, pp. 568.

Ramsay, J.G., Huber, M.I., 1987. Modern Structural Geology. In: Folds and Fractures, vol. 2. Academic Press, London.

Timoshenko, S., 1940. Strength of Materials. D. Van Nostrand Company, New York.

Toimil, N.C., 2005. Geometría y patrones de deformación en pliegues simétricos desarrollados en capas competentes. Unpublished thesis, Universidad de Oviedo.

Zhang, Y., Mancktelow, N.S., Hobbs, B.E., Ord, A., Mühlhaus, H.B., 2000. Numerical modelling of single layer folding: clarification of an issue regarding the possible effect of computer codes and the influence of initial irregularities. Journal of Structural Geology 22, 1511–1522.